

The Inverse Dynamics of a 3-DOF Parallel Mechanism Based on Analytical Forward Kinematics

Ke Wang

Changzhou University

Ju Li

Changzhou University

Huiping Shen (✉ shp65@126.com)

Changzhou University <https://orcid.org/0000-0002-1563-0924>

Jingjing You

Nanjing Forestry University

Ting-Li Yang

Changzhou University

Original Article

Keywords: parallel mechanism, dynamic model, Newton-Euler method, simulation verification

Posted Date: August 13th, 2020

DOI: <https://doi.org/10.21203/rs.3.rs-57314/v1>

License:   This work is licensed under a Creative Commons Attribution 4.0 International License.

[Read Full License](#)

The Inverse Dynamics of a 3-DOF Parallel Mechanism Based on Analytical Forward Kinematics

Ke Wang, born in 1994, is currently a engineer at *Black & Decker(Suzhou) Technology Limited Company, China*. He received his master degree from *Changzhou University, China*, in 2020.
E-mail: wangk1994@163.com

Ju Li, born in 1981, is currently a Vice Professor at *Changzhou University, China*. Her main research interests include parallel mechanism, kinematics, E-mail: wangju0209@163.com

Huiping Shen, born in 1965, is currently a Professor and a PhD candidate supervisor at *Changzhou University, China*. His main research interests include parallel mechanism, kinematics, topology.
E-mail: shp65@126.com

Jingjing You, born in 1985, is currently a Vice Professor and a Master supervisor at *College of Mechanical and Electronic Engineering, Nanjing Forestry University, China*. E-mail: youjingjing251010@126.com

Ting-Li Yang, born in 1940, is currently a Guest Professor. His main research interest include modern mechanisms, basic theory of robotic mechanisms. E-mail: yangti@126.com

Corresponding author: Huiping Shen E-mail: shp65@126.com

The Inverse Dynamics of a 3-DOF Parallel Mechanism Based on Analytical Forward Kinematics

Ke Wang¹ • Ju Li¹ • Huiping Shen^{1*} • Jingjing You² • Ting-li Yang¹

Received on xx xx, 2020; accepted on xx xx, 2020

Abstract: A new type of 3-dof parallel mechanism (PM) with analytical forward displacement analysis is proposed. The reverse dynamic equation of the PM is solved. Different from the traditional dynamic analysis using inverse kinematics, the displacement, velocity and acceleration equations of the PM are established and solved by forward kinematics. The inverse dynamic equation of the PM is constructed and solved by analyzing the forces on each link and based on Newton-Euler method. The correctness of the dynamic model is verified by an example using MATLAB and ADAMS. The maximum driving force error of each actuated pair is 1.32%, 5.8% and 5.2% respectively. This paper provides a theoretical basis for the design, manufacture and application of the PM.

Keywords: parallel mechanism • dynamic model • Newton-Euler method • simulation verification

1 Introduction¹

Compared with the series mechanism, the parallel mechanism (PM) has the advantages of compact structure, high rigidity and motion accuracy, etc., The topic has attracted extensive attention from the academic and industrial community for many years [1-3]. At present, research on PMs mainly focuses on the topology, kinematics, dynamics and control [4-6]. The dynamic analysis mainly studies the relationship between the input forces and the output forces. This is the determination of the maximum load carrying capacity and reasonable design of the driver during the development of parallel robots. According to this, the constraint reaction force of the motion pair solved during the analysis process plays an important role in the design, mechanical efficiency estimation, friction calculation, and

mechanical vibration research of the various parts of the PM. Therefore, for a PM to be developed, it is necessary to establish a dynamic model that can accurately and meet the requirements of real-time control.

In terms of modeling methods, the commonly used dynamic modeling methods are Lagrangian method, universal equations of dynamics, Newton-Euler method, etc. [7-9]. Among them, the universal equations of dynamics and Lagrange method are based on the system's virtual displacement and kinetic and potential energy respectively to build a simple dynamic model. While the Newton-Euler method can obtain the force of each joint by analyzing each member separately, and then establishes a complete dynamic model by eliminating the interaction force of each member [10], it can also solve the support force and moment of force between members.

In terms of research objects, most of the kinetic analysis mainly focus on the 6-DOF Stewart PM [11-13]. For 5-DOF PM, Chen et.al [14] use the universal equations of dynamics to analyze the 4-UPS-UPU PM. Li et.al [10] used the Newton-Euler method to analyze the dynamics of the 5-PSS / UPU PM. For 4-DOF PM, Geng [15] used Newton-Euler to analyze the 4UPS-UPR PM. In terms of 3-DOF, Li et.al [16] used the Newton-Euler method to analyze the dynamics of a 3-RPS PM. Liu et.al [17] performed a Lagrangian method to analyze the dynamics of a 3-RRS PM.

In this paper, a 3-DOF 2T1R PM [18] with a forward analytical position solution is proposed. Firstly, the kinematics of the PM is analyzed. Then, force analysis is carried out for each component, and the dynamic model is established by Newton-Euler method. Finally, the correctness of the modeling method is verified by comparing the results of Matlab calculation and ADAMS simulation. It provides the theoretical basis of mechanics for the design, manufacture and application of the PM.

✉ Huiping Shen
Shp65@126.com

¹ School of Mechanical Engineering, Changzhou University, Changzhou 213164, China

² College of Mechanical and Electronic Engineering, Nanjing Forestry University, Nanjing 210037, China

2 Mechanism architecture

The PM shown in Figure 1 consists of a moving platform, a base, and a complex branch chain and an unconstrained branch PSS (Prismatic pair - Spherical joint - Spherical joint) connecting the moving platform and the base. The sub-PM and an revolute pair are connected in series, where the two branches of the sub-PM are SOC₁ $\{-P \perp P^{(4R)}-\}$, SOC₂ $\{-P \perp R \parallel R\}$, where $P^{(4R)}$ indicates that a parallelogram composed of 4 revolute pairs that is equivalent to a prismatic pair P , while SOC means single-open-chain that consists of link and pair in serial way. This PM can generate two translations in the Y and Z directions and a rotation output about the Y axis. The PM is referred to as the 2T1R PM [18].

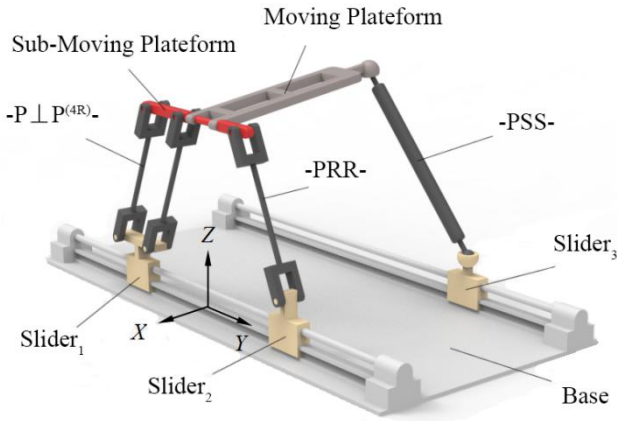


Figure 1 3D model of a 2T1R PM

2.1 Kinematics analysis

The coordinate system shown in Figure 2 is established. The base coordinate system $O-XYZ$ is established with the origin at the center point O of the guide rail where the driving pair A_1 , A_2 is located, the positive half of the Y -axis is from O to A_2 , and the positive half of the Z -axis is vertical upward. The moving coordinate system $o-xyz$ is established with the origin at o point that is the center point O of the line $C_{12}C_2$ on the sub-moving platform. The positive half of the y -axis is from the origin o to C_2 , and the z -axis is perpendicular to the plane of the moving platform. While the X and x axis direction meet the right-hand screw rule, the geometry parameters of each component are shown in Figure 2.

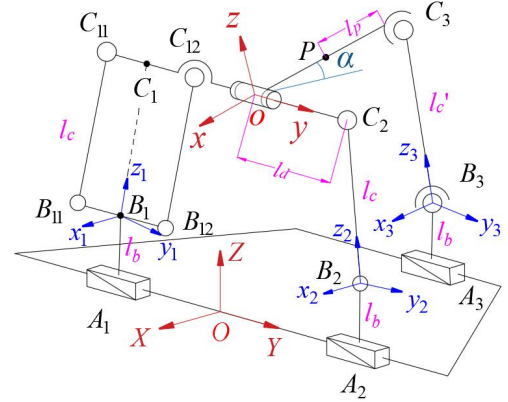


Figure 2 Schematic diagram of 2T1R PM

Establish the local coordinate system of each link B_iC_i ($i=1,2,3$). The x_1 axis of the coordinate system $B_1-x_1y_1z_1$ is parallel to the X axis of the base coordinate system, and the positive half of the z_1 axis is pointed from B_1 to C_1 ; The x_2 axis of the coordinate system $B_2-x_2y_2z_2$ is parallel to the X axis of the base coordinate system, and the positive half of the z_2 axis is pointed from B_2 to C_2 , where the y axis of each coordinate system meets the right-hand screw rule; The positive half of the z_3 axis of the coordinate system $B_3-x_3y_3z_3$ is pointed from B_3 to C_3 , and the x_3 axis lies in the XOZ plane and the angle with the X axis is θ_1 , its Euler transformation relative to the base coordinate system is shown in Figure 3, from which the coordinate transformation matrix from the coordinate system $\{B_3\}$ to the base coordinate system $O-XYZ$ is:

$${}^O R_{i_3} = R(Y, \theta_1) R(x_3', \theta_2)$$

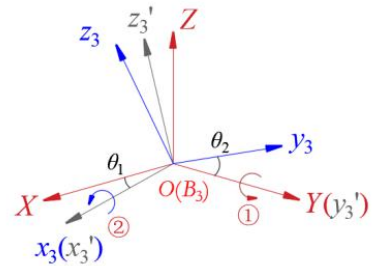


Figure 3 Coordinate system $B_3 - x_3y_3z_3$ Euler transform

2.2 Forward Position Solution

The forward kinematics of PM is to solve the position and orientation of the moving platform when the structural parameters and input of the mechanism are given.

Based on the constrained length of the bars, we can get:

$$\begin{aligned}
f_1: l_c^2 - (z - l_b)^2 - (y - l_d - l_1)^2 &= 0 \\
f_2: l_c^2 - (z - l_b)^2 - (l_2 - y - l_d)^2 &= 0 \\
f_3: (-2l_p \cos \alpha - x_{A_3})^2 + (y - l_3)^2 + (z + 2l_p \sin \alpha - l_b)^2 &= l_c'^2
\end{aligned} \quad (1)$$

From Eq. (1), the coordinates of point o are:

$$\begin{aligned}
y &= \frac{l_1 + l_2}{2} \\
z &= \sqrt{l_c'^2 - \left(\frac{l_2 - l_1}{2} - l_d\right)^2} + l_b
\end{aligned} \quad (2)$$

Angle α of moving platform is:

$$\alpha = 2 \arctan \left(\frac{-B \pm \sqrt{B^2 - C^2 + A^2}}{C - A} \right) \quad (3)$$

where,

$$\begin{aligned}
A &= 4(z - l_b) \cdot l_p \\
B &= 4x_{A_3} \cdot l_p \\
C &= -4l_p'^2 - x_{A_3}^2 - (y - l_3)^2 - (z - l_b)^2 + l_c'^2
\end{aligned}$$

2.3 Velocity and acceleration analysis

2.3.1 Velocity and acceleration of the moving platform

Taking the time derivative of Eq. (2) ~ (3), the output velocity and acceleration of the moving platform can be obtained as

$$\begin{aligned}
\dot{\chi} &= [\dot{y} \quad \dot{z} \quad \dot{\alpha}]^T \\
\ddot{\chi} &= [\ddot{y} \quad \ddot{z} \quad \ddot{\alpha}]^T
\end{aligned}$$

2.3.2 Velocity and acceleration of members

(1) Velocity and acceleration of member B_1C_1

Because the movements of the $B_{11}C_{11}$ and $B_{12}C_{12}$ rods are the same, the two rods are equivalent to the rod B_1C_1 for analysis.

The velocity of the point C_1 is:

$$\mathbf{v}_{c_1} = \mathbf{v}_o = \mathbf{v}_1 + \boldsymbol{\omega}_{l_1} \times \mathbf{c}_1 \cdot l_c \quad (4)$$

Where, \mathbf{v}_o is the linear velocity of point o ; \mathbf{v}_1 is the linear velocity of the driving pair A_1 ; \mathbf{c}_1 and $\boldsymbol{\omega}_{l_1}$ are respectively the linear and angular velocity of the rod B_1C_1 .

The angular velocity of the rod B_1C_1 can be determined by taking the cross product of the two sides of Eq.(4) with \mathbf{c}_1 , which yields:

$$\boldsymbol{\omega}_{l_1} = \frac{\mathbf{c}_1 \times (\mathbf{v}_{c_1} - \mathbf{v}_1)}{l_c} \quad (5)$$

Substituting Eq.(5) into Eq.(6) to obtain the velocity of the center of mass of the rod B_1C_1 ,

$$\mathbf{v}_{l_1} = \mathbf{v}_1 + \boldsymbol{\omega}_{l_1} \times \mathbf{c}_1 \cdot \frac{l_c}{2} \quad (6)$$

Taking the time derivative of Eq. (4), the acceleration of the C_1 can be obtained as:

$$\mathbf{a}_{c_1} = \mathbf{a}_o = \mathbf{a}_1 + \boldsymbol{\varepsilon}_{l_1} \times \mathbf{c}_1 \cdot l_c + \boldsymbol{\omega}_{l_1} \times (\boldsymbol{\omega}_{l_1} \times \mathbf{c}_1) \cdot l_c \quad (7)$$

The angular acceleration of the rod B_1C_1 can be determined by taking the cross product of the two sides of Eq.(7) with \mathbf{c}_1 , which yields:

$$\boldsymbol{\varepsilon}_{l_1} = \frac{\mathbf{c}_1 \times (\mathbf{a}_o - \mathbf{a}_1)}{l_c} = \tilde{\mathbf{c}}_1 \cdot (\mathbf{a}_o - \mathbf{a}_1) \quad (8)$$

Where, $\tilde{\mathbf{c}}_1$ is the skew symmetric matrix associated with the vector \mathbf{c}_1 .

Taking the time derivative of Eq. (4), the centroid acceleration of rod B_1C_1 can be obtained as:

$$\mathbf{a}_{l_1} = \mathbf{a}_1 + \boldsymbol{\varepsilon}_{l_1} \times \mathbf{c}_1 \cdot \frac{l_c}{2} + \boldsymbol{\omega}_{l_1} \times \frac{l_c}{2} (\boldsymbol{\omega}_{l_1} \times \mathbf{c}_1) = \frac{1}{2} (\mathbf{a}_1 + \mathbf{a}_o) \quad (9)$$

(2) Velocity and acceleration of member B_2C_2

Similarly, using the same method as the velocity and acceleration of the rod B_1C_1 , the angular velocity of the rod B_2C_2 can be obtained as:

$$\boldsymbol{\omega}_{l_2} = \frac{\mathbf{c}_2 \times (\mathbf{v}_{c_2} - \mathbf{v}_2)}{l_c} \quad (10)$$

The centroid velocity of the rod B_2C_2 :

$$\mathbf{v}_{l_2} = \mathbf{v}_2 + \boldsymbol{\omega}_{l_2} \times \mathbf{c}_2 \cdot \frac{l_c}{2} \quad (11)$$

Angular acceleration of rod B_2C_2 :

$$\boldsymbol{\varepsilon}_{l_2} = \frac{\mathbf{c}_2 \times (\mathbf{a}_o - \mathbf{a}_2)}{l_c} = \tilde{\mathbf{c}}_2 \cdot (\mathbf{a}_o - \mathbf{a}_2) \quad (12)$$

Centroid acceleration of rod B_2C_2 :

$$\mathbf{a}_{l_2} = \mathbf{a}_2 + \boldsymbol{\varepsilon}_{l_2} \times \mathbf{c}_2 \cdot \frac{l_c}{2} + \boldsymbol{\omega}_{l_2} \times \frac{l_c}{2} (\boldsymbol{\omega}_{l_2} \times \mathbf{c}_2) = \frac{1}{2} (\mathbf{a}_2 + \mathbf{a}_o) \quad (13)$$

(3) Velocity and acceleration of rod B_3C_3

The velocity of the point C_3 is

$$\mathbf{v}_{c_3} = \mathbf{v}_o + \boldsymbol{\omega}_o \times \mathbf{c}_p = \mathbf{v}_3 + \boldsymbol{\omega}_{l_3} \times \mathbf{c}_3 \cdot l_c' \quad (14)$$

The angular velocity of the rod B_3C_3 can be determined by taking the cross product of the two sides of Eq.(14) with \mathbf{c}_3 , which yields:

$$\boldsymbol{\omega}_{l_3} = \frac{\mathbf{c}_3 \times (\mathbf{v}_{c_3} - \mathbf{v}_3)}{l_c'} \quad (15)$$

Substituting Eq.(15) into Eq.(16) gives the velocity at the centroid of rod B_3C_3 :

$$\mathbf{v}_{l_3} = \mathbf{v}_3 + \boldsymbol{\omega}_{l_3} \times \mathbf{c}_3 \cdot \frac{l_c'}{2} \quad (16)$$

Taking the time derivative of Eq. (14), the acceleration of the C_3 can be obtained as:

$$\begin{aligned} \mathbf{a}_{c_3} &= \mathbf{a}_o + \boldsymbol{\varepsilon}_o \times \mathbf{c}_p + \boldsymbol{\omega}_o \times (\boldsymbol{\omega}_o \times \mathbf{c}_p) \\ &= \mathbf{a}_3 + \boldsymbol{\varepsilon}_{l_3} \times \mathbf{c}_3 \cdot l_c' + \boldsymbol{\omega}_{l_3} \times (\boldsymbol{\omega}_{l_3} \times \mathbf{c}_3) l_c' \end{aligned} \quad (17)$$

The angular acceleration of the rod B_3C_3 can be determined by taking the cross product of the two sides of Eq.(17) with \mathbf{c}_3 , which yields:

$$\boldsymbol{\varepsilon}_{l_3} = \frac{\mathbf{c}_3 \times (\mathbf{a}_{c_3} - \mathbf{a}_3)}{l_c'} = \frac{\tilde{\mathbf{c}}_3 \cdot (\mathbf{a}_{c_3} - \mathbf{a}_3)}{l_c'} \quad (18)$$

Taking the time derivative of Eq. (16), the acceleration of the centroid of B_3C_3 can be obtained as:

$$\mathbf{a}_{l_3} = \mathbf{a}_3 + \boldsymbol{\varepsilon}_{l_3} \times \mathbf{c}_3 \cdot \frac{l_c'}{2} + \boldsymbol{\omega}_{l_3} \times \frac{l_c'}{2} (\boldsymbol{\omega}_{l_3} \times \mathbf{c}_3) = \frac{1}{2} (\mathbf{a}_3 + \mathbf{a}_{c_3}) \quad (19)$$

3 Dynamics modeling of mechanism

When using the Newton-Euler method, the friction of each moving pair is not considered, then the Newton-Euler equation of each member is established. Then the dynamic model of the PM is obtained by eliminating the internal forces between the members. Finally, the relationship between the driving force and the external forces of the moving platform is obtained, which is illustrated as follows.

3.1 Dynamic equation of moving platform

As shown in Figure 4, the gravity of the moving platform is $m\mathbf{g}$, the constraint force of the sub-moving platform is \mathbf{F}_{a1} , and the constraint force of the PSS branch chain is \mathbf{F}_{a2} . The external force and moment of the moving platform are \mathbf{F}_w and \mathbf{M}_w , respectively.

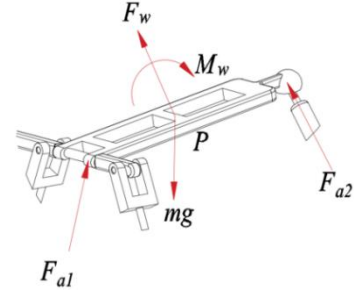


Figure 4 Force analysis of the moving platform

The dynamic equation of the moving platform is:

$$\mathbf{F}_w + \mathbf{F}_{a1} + \mathbf{F}_{a2} + m\mathbf{g} = m\mathbf{a}_p \quad (20)$$

$$\mathbf{M}_w - \frac{1}{2} \mathbf{c}_p \times \mathbf{F}_{a1} + \frac{1}{2} \mathbf{c}_p \times \mathbf{F}_{a2} = {}^o\mathbf{I}_p \boldsymbol{\varepsilon}_p + \boldsymbol{\omega}_p \times ({}^o\mathbf{I}_p \boldsymbol{\omega}_p) \quad (21)$$

Where, ${}^o\mathbf{I}_p = {}^o\mathbf{R}_p \mathbf{I}_p {}^o\mathbf{R}_p^T$; ${}^o\mathbf{R}_p$ is the transformation matrix of the moving coordinate system to the base coordinate system; ${}^o\mathbf{I}_p$ is the inertia tensor of the moving platform in the base frame; \mathbf{I}_p is the inertia tensor of the moving platform in the local frame; \mathbf{c}_p is the position vector from the center of mass of the moving platform to the center of the spherical joint on the moving platform.

3.2 Dynamic equation of the sub-moving platform

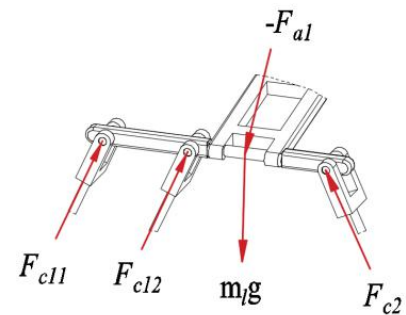


Figure 5 Force analysis of sub-moving platform

As shown in Figure 5, the dynamic equation of the sub-moving platform can be written as follows:

$$-\mathbf{F}_{a1} + m_l \mathbf{g} + \mathbf{F}_{c11} + \mathbf{F}_{c12} + \mathbf{F}_{c2} = m_l \mathbf{a}_o \quad (22)$$

Where \mathbf{F}_{c11} , \mathbf{F}_{c12} , \mathbf{F}_{c2} are constraint forces of the active link $B_i C_i$ ($i=1,2$) in the sub-moving platform; m_l is mass of the

sub-moving platform; $-\mathbf{F}_{a1}$ is the reaction force of the moving platform.

3.3 Dynamic equation of connecting rod

The R-R-link is subject to the constraint reaction force of the sub-moving platform $-\mathbf{F}_{ci}$ ($i=1,2$), its own gravity $m_c\mathbf{g}$, and the constraint force \mathbf{F}_{bi} ($i = 1,2$), and its force analysis is shown in Figure 6.

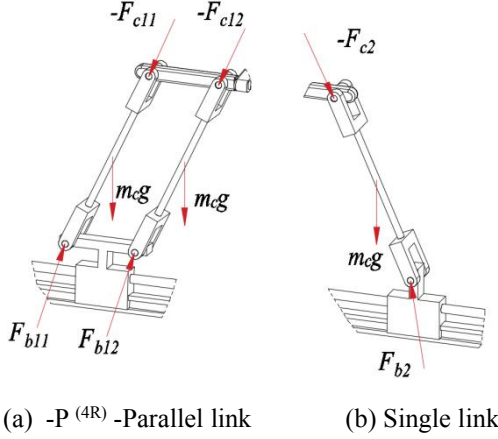


Figure 6 Force analysis of -R-R-link

Therefore, the dynamic equations of the two parallel links in the parallelogram are as follows.

$$-\mathbf{F}_{c1i} + m_c \mathbf{g} + \mathbf{F}_{b1i} = m_c \mathbf{a}_{1i}, (i = 1,2) \quad (23)$$

$$\frac{l_c}{2} \mathbf{c}_i \times (-\mathbf{F}_{ci}) + \frac{l_c}{2} (-\mathbf{c}_i) \times \mathbf{F}_{bi} = {}^o\mathbf{I}_{li} \boldsymbol{\varepsilon}_{li} + \boldsymbol{\omega}_{li} \times ({}^o\mathbf{I}_{li} \boldsymbol{\omega}_{li}) \quad (24)$$

Dynamic equation of single link (B_2C_2) is as follows.

$$-\mathbf{F}_{c2} + m_c \mathbf{g} + \mathbf{F}_{b2} = m_c \mathbf{a}_{12} \quad (25)$$

$$\frac{l_c}{2} \mathbf{c}_2 \times (-\mathbf{F}_{c2}) + \frac{l_c}{2} (-\mathbf{c}_2) \times \mathbf{F}_{b2} = {}^o\mathbf{I}_{l2} \boldsymbol{\varepsilon}_{l2} + \boldsymbol{\omega}_{l2} \times ({}^o\mathbf{I}_{l2} \boldsymbol{\omega}_{l2}) \quad (26)$$

Where, ${}^o\mathbf{I}_{li} = {}^o\mathbf{R}_{li} \mathbf{I}_{li} {}^o\mathbf{R}_{li}^T$ ($i=1,2$), ${}^o\mathbf{I}_{li}$ is the inertia tensor of the connecting rod in the base frame; \mathbf{I}_{li} is the inertia tensor of the connecting rod in the local frame; ${}^o\mathbf{R}_{li}$ is the transformation matrix from the local frames of the connecting rod to the base frame.

Further, -S-S-link (B_3C_3) is subject to the constraint reaction force of the moving platform $-\mathbf{F}_{a2}$, the constraint force of the drive member \mathbf{F}_{b3} , the self-gravity $m_c'\mathbf{g}$, while m_c' is the mass of -S-S- connecting rod, and its stress is shown in Figure 7.

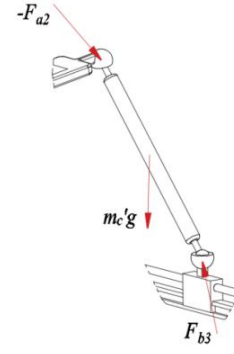


Figure 7 Force analysis diagram of -S-S- Link

Then, the dynamic equations of the -S-S- link are described as

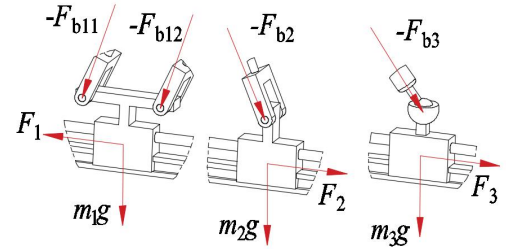
$$-\mathbf{F}_{a2} + m_c' \mathbf{g} + \mathbf{F}_{b3} = m_c' \mathbf{a}_{13} \quad (27)$$

$$\frac{l_c'}{2} \mathbf{c}_3 \times (-\mathbf{F}_{a2}) + \frac{l_c'}{2} (-\mathbf{c}_3) \times \mathbf{F}_{b3} = {}^o\mathbf{I}_{l3} \boldsymbol{\varepsilon}_{l3} + \boldsymbol{\omega}_{l3} \times ({}^o\mathbf{I}_{l3} \boldsymbol{\omega}_{l3}) \quad (28)$$

where, ${}^o\mathbf{I}_{l3} = {}^o\mathbf{R}_{l3} \mathbf{I}_{l3} {}^o\mathbf{R}_{l3}^T$.

3.4 Dynamic equation of driving sliders

The three driving sliders are subject to the constraint reaction forces of each link- \mathbf{F}_{bi} ($i = 1,2,3$), its own gravity, and the driving force of the driving motor $m_i \mathbf{g}$ ($i = 1,2,3$), and the force diagram of the slider is shown in Figure 8.



(a) Slider 1 (A_1) (b) Slider 2 (A_2) (c) Slider 3 (A_3)

Figure 8 Force analysis of three drive sliders

The dynamic equation of slider 1 is

$$\mathbf{F}_1 - \mathbf{F}_{b11} - \mathbf{F}_{b12} + m_1 \mathbf{g} = m_1 \mathbf{a}_1 \quad (29)$$

The dynamic equations of slider 2 and slider 3 are as follows.

$$\mathbf{F}_i - \mathbf{F}_{bi} + m_i \mathbf{g} = m_i \mathbf{a}_i, (i = 2,3) \quad (30)$$

3.5 The integrated dynamic model of the PM

The establishment of the integrated dynamic model is to eliminate the internal forces of members and to obtain the dynamic relationship between the input force, torque and output force.

Taking the dot product of the both sides of Eq(29) with \mathbf{e}_1^T

$$\tau_1 = \mathbf{e}_1^T \cdot \mathbf{F}_1 = \mathbf{e}_1^T \cdot (\mathbf{F}_{b11} + \mathbf{F}_{b12}) + m_1 a_1 \quad (31)$$

Where, $\tau_i (i = 1, 2, 3)$ is the driving force of the slider, $\mathbf{e}_i (i = 1, 2, 3)$ is the unit vector for driving force.

Substituting Eq. (23) into Eq. (31), we can write:

$$\tau_1 = \mathbf{e}_1^T \cdot \sum_{i=1}^2 (\mathbf{F}_{c1i} - m_c \mathbf{g} + m_c \mathbf{a}_{1i}) + m_1 a_1 \quad (32)$$

According to Eq.(24),we can write:

$$l_c \mathbf{c}_1 \times (\mathbf{F}_{c11} + \mathbf{F}_{c12}) = \mathbf{C}_1 \quad (33)$$

$$\mathbf{C}_1 = l_c \mathbf{c}_1 \times (m_c \mathbf{g} - m_c \mathbf{a}_{11}) - 2 {}^o \mathbf{I}_{11} \boldsymbol{\varepsilon}_{11} - 2 \boldsymbol{\omega}_{11} \times ({}^o \mathbf{I}_{11} \boldsymbol{\omega}_{11}) \quad (34)$$

Taking the cross product of the two sides of Eq.(33) with \mathbf{e}_1 gives:

$$l_c \mathbf{e}_1 \times \mathbf{c}_1 \times (\mathbf{F}_{c11} + \mathbf{F}_{c12}) = \mathbf{e}_1 \times \mathbf{C}_1 \quad (35)$$

Then,we can write:

$$\mathbf{F}_{c11} + \mathbf{F}_{c12} = \frac{\mathbf{c}_1 [\mathbf{e}_1^T (\mathbf{F}_{c11} + \mathbf{F}_{c12})]}{\mathbf{e}_1^T \cdot \mathbf{c}_1} - \frac{\mathbf{e}_1 \times \mathbf{C}_1}{l_c \mathbf{e}_1^T \mathbf{c}_1} \quad (36)$$

According to Eq.(32), we can get:

$$\mathbf{e}_1^T (\mathbf{F}_{c11} + \mathbf{F}_{c12}) = \tau_1 + 2 \mathbf{e}_1^T (m_c \mathbf{g} - m_c \mathbf{a}_{11}) - m_1 a_1 \quad (37)$$

Substituting Eq. (37) into Eq. (36) gives:

$$\mathbf{F}_{c11} + \mathbf{F}_{c12} = \frac{\mathbf{c}_1 [\tau_1 + 2 \mathbf{e}_1^T (m_c \mathbf{g} - m_c \mathbf{a}_{11}) - m_1 a_1]}{\mathbf{e}_1^T \cdot \mathbf{c}_1} - \frac{\mathbf{e}_1 \times \mathbf{C}_1}{l_c \mathbf{e}_1^T \mathbf{c}_1} \quad (38)$$

Similarly,

$$\mathbf{F}_{c2} = \frac{\mathbf{c}_2 [\tau_2 + \mathbf{e}_2^T (m_c \mathbf{g} - m_c \mathbf{a}_{12}) - m_2 a_2]}{\mathbf{e}_2^T \cdot \mathbf{c}_2} - \frac{\mathbf{e}_2 \times \mathbf{C}_2}{l_c \mathbf{e}_2^T \mathbf{c}_2} \quad (39)$$

$$\mathbf{F}_{c3} = \frac{\mathbf{c}_3 [\tau_3 + \mathbf{e}_3^T (m_c \mathbf{g} - m_c \mathbf{a}_{13}) - m_3 a_3]}{\mathbf{e}_3^T \cdot \mathbf{c}_3} - \frac{\mathbf{e}_3 \times \mathbf{C}_3}{l_c \mathbf{e}_3^T \mathbf{c}_3} \quad (40)$$

where,

$$\mathbf{C}_2 = l_c \mathbf{c}_2 \times (m_c \mathbf{g} - m_c \mathbf{a}_{12}) - {}^o \mathbf{I}_{12} \boldsymbol{\varepsilon}_{12} - \boldsymbol{\omega}_{12} \times ({}^o \mathbf{I}_{12} \boldsymbol{\omega}_{12})$$

$$\mathbf{C}_3 = l_c \mathbf{c}_3 \times (m_c \mathbf{g} - m_c \mathbf{a}_{13}) - {}^o \mathbf{I}_{13} \boldsymbol{\varepsilon}_{13} - \boldsymbol{\omega}_{13} \times ({}^o \mathbf{I}_{13} \boldsymbol{\omega}_{13})$$

Substituting Eqs. (38) and (39) into Eq. (22), we can get

$$\mathbf{F}_{a1} = m_1 \mathbf{g} + \mathbf{F}_{c11} + \mathbf{F}_{c12} + \mathbf{F}_{c2} - m_1 \mathbf{a}_o \quad (41)$$

Substituting Eqs. (40) and (41) into Eq. (20) and Eq. (21), we have

$$\begin{bmatrix} \mathbf{D} \\ \mathbf{E} \end{bmatrix}_{6 \times 1} = \mathbf{J}_\tau \cdot \boldsymbol{\tau} + \begin{bmatrix} \mathbf{F}_w \\ \mathbf{M}_w \end{bmatrix}_{6 \times 1} \quad (42)$$

where

$$\mathbf{D} = -\frac{\mathbf{c}_1 [2 \mathbf{e}_1^T (m_c \mathbf{g} - m_c \mathbf{a}_{11}) - m_1 a_1]}{\mathbf{e}_1^T \mathbf{c}_1} - \frac{\mathbf{c}_2 [2 \mathbf{e}_2^T (m_c \mathbf{g} - m_c \mathbf{a}_{12}) - m_2 a_2]}{\mathbf{e}_2^T \mathbf{c}_2}$$

$$+ \sum_{i=1}^2 \frac{\mathbf{e}_i \times \mathbf{C}_i}{l_c \mathbf{e}_i^T \mathbf{c}_i} - \frac{\mathbf{c}_3 [2 \mathbf{e}_3^T (m_c \mathbf{g} - m_c \mathbf{a}_{13}) - m_3 a_3]}{\mathbf{e}_3^T \mathbf{c}_3} + \frac{\mathbf{e}_3 \times \mathbf{C}_3}{l_c \mathbf{e}_3^T \mathbf{c}_3} - m_1 (\mathbf{g} - \mathbf{a}_o)$$

$$- m (\mathbf{g} - \mathbf{a}_p)$$

$$\mathbf{E} = \frac{1}{2} c_p \times \left[\frac{\mathbf{c}_1 [2 \mathbf{e}_1^T (m_c \mathbf{g} - m_c \mathbf{a}_{11}) - m_1 a_1]}{\mathbf{e}_1^T \mathbf{c}_1} + \frac{\mathbf{c}_2 [2 \mathbf{e}_2^T (m_c \mathbf{g} - m_c \mathbf{a}_{12}) - m_2 a_2]}{\mathbf{e}_2^T \mathbf{c}_2} \right]$$

$$- \sum_{i=1}^2 \frac{\mathbf{e}_i \times \mathbf{C}_i}{l_c \mathbf{e}_i^T \mathbf{c}_i} + m_1 (\mathbf{g} - \mathbf{a}_o) - \frac{1}{2} c_p \times \left[\frac{\mathbf{c}_3 [2 \mathbf{e}_3^T (m_c \mathbf{g} - m_c \mathbf{a}_{13}) - m_3 a_3]}{\mathbf{e}_3^T \mathbf{c}_3} - \frac{\mathbf{e}_3 \times \mathbf{C}_3}{l_c \mathbf{e}_3^T \mathbf{c}_3} \right] -$$

$${}^o \mathbf{I}_p \boldsymbol{\varepsilon}_p - \boldsymbol{\omega}_p \times ({}^o \mathbf{I}_p \boldsymbol{\omega}_p)$$

$$\mathbf{J}_\tau = \begin{bmatrix} \frac{\mathbf{c}_1}{\mathbf{e}_1^T \mathbf{c}_1} & \frac{\mathbf{c}_2}{\mathbf{e}_2^T \mathbf{c}_2} & \frac{\mathbf{c}_3}{\mathbf{e}_3^T \mathbf{c}_3} \\ -\frac{\mathbf{c}_p \times \mathbf{c}_1}{2 \mathbf{e}_1^T \mathbf{c}_1} & -\frac{\mathbf{c}_p \times \mathbf{c}_2}{2 \mathbf{e}_2^T \mathbf{c}_2} & \frac{\mathbf{c}_p \times \mathbf{c}_3}{2 \mathbf{e}_3^T \mathbf{c}_3} \end{bmatrix}_{6 \times 3}$$

$$\boldsymbol{\tau} = [\tau_1 \quad \tau_2 \quad \tau_3]^T_{3 \times 1}$$

According to Eq. (42), we can get:

$$\boldsymbol{\tau} = \mathbf{J}_\tau^{-1} \cdot \begin{bmatrix} \mathbf{D} \\ \mathbf{E} \end{bmatrix} - \mathbf{J}_\tau^{-1} \cdot \begin{bmatrix} \mathbf{F}_w \\ \mathbf{M}_w \end{bmatrix} \quad (43)$$

When the motion law of the moving platform and the external force and torque are known, the driving force of each driving pair can be obtained from Eq.(43).

4 Dynamic Simulation

Firstly, the following motion laws of three driving pairs are given.

$$\begin{cases} l_1 = 10 \cos(t) - 27 \\ l_2 = -10 \cos(t) + 27 \\ l_3 = -10 \cos(t) + 14 \end{cases} \quad (44)$$

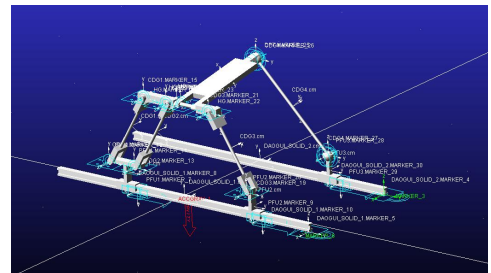


Figure 9 Virtual prototype of 2T1R parallel mechanism

A three-dimensional prototype of the PM is designed, as shown in Figure 9. The dimension parameters of the PM are shown in Table 1.

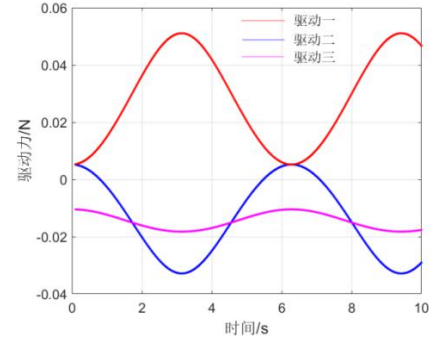
Table 1 Dimension Parameters of the 2T1R PM

Size parameters	Value
l_b / mm	10
l_d / mm	17
l_c / mm	43.8
l_c' / mm	60
$-XA_3 / \text{mm}$	60
$2lp / \text{mm}$	54
m_1 / kg	0.00254
m_2 / kg	0.00162
m_3 / kg	0.00153
m_c / kg	0.00285
m_c' / kg	0.00129
m_l / kg	0.00491
m / kg	0.0131

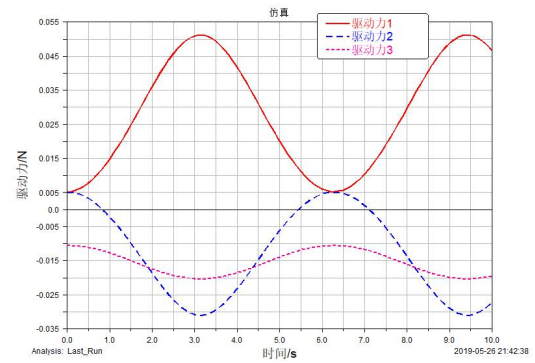
The above parameters are substituted into the dynamic Eqs.(20) ~ (43), and the driving forces of the three driving pairs are calculated by MATLAB. The curves of the driving forces are shown in Figure 10 (a).

Then, the three-dimensional prototype is input into ADAMS, and the material properties of each part and the constraint types of the kinematic pairs are specified. The vertical downward gravity is applied, and the simulation step of 0.01s and the simulation time of 10s are selected for dynamic simulation of the virtual prototype.

As shown in Fig.10 (b), the calculated value is compared with the simulation result of ADAMS, which shows that the simulation value is basically consistent with the theoretical value. The maximum error of the driving force of each pair is 1.32%, 5.8% and 5.2%, which verifies the correctness of the dynamic model.



(a) Theoretical driving force



(b) Driving force simulation value

Figure 10 Driving Force of Each Driving Pair

Under the same simulation duration, different steps are selected to record the calculation time of MATLAB, as shown in Table 2.

Table 2 Matlab calculation time

Simulation duration / s	Step size / s	Calculation time / s
10	0.01	4.77
10	0.005	9.13
10	0.004	11.64

As shown in Table 2, only when the step size $\leq \frac{10}{0.005} = 2000$, the dynamic modeling analysis program is real-time.

5 Conclusions

For a new type of 3-DOF PM proposed in this paper, the analytical solution of forward kinematics is given, and it is used to analyze the velocity and acceleration. The driving force is obtained by calculating the dynamic equation. The dynamic simulation of the three-dimensional prototype is

carried out by ADAMS, and the simulation value of driving force is obtained. By comparing the two cases, the correctness of the dynamic modeling is verified, which lays a foundation for the design, manufacture and application of PM.

6 Declaration

Acknowledgement

The first authors sincerely thanks to Professor Shen of Changzhou University for his critical discussion and reading during manuscript preparation.

Funding

Supported by National Natural Science Foundation of China (Grant No.51975062) and National Science Foundation of Jiangsu Province (Grant No.BK20161192)

Availability of data and materials

The datasets supporting the conclusions of this article are included within the article.

Authors' contributions

The author' contributions are as follows: Huiping Shen was in charge of the whole work; Ke Wang wrote the manuscript.

Competing interests

The authors declare no competing financial interests.

Consent for publication

Yes

Ethics approval and consent to participate

Yes

References

- [1] H P Shen, M Lv, X R Zhu, Y F Li. Topological design and kinematics of a single-degree-of-freedom 3T1R parallel mechanism [J]. *China Mechanical Engineering*, 2019, 30 (08): 961-968.
- [2] T L Yang, A X Liu, H P Shen, et al. Topological Design of Robot Mechanism. Beijing: Science Press, 2012.05.
- [3] B Y Chang, X N Li, G G Jin, Z Zhang, S Yang. Kinematics analysis of a 3T1R parallel mechanism with full-circle rotation capability [J]. *Journal of Agricultural Machinery*, 2019, 50(7): 406-416.
- [4] Moussab Bennehar, Ahmed Chemori, François Pierrot. A new revised desired compensation adaptive control for enhanced tracking: application to RA-PKMs[J]. *Advanced Robotics*, 2016, 30(17-18): 1192-1214.
- [5] H P Shen, K Xu, T L Yang, J M Deng. Design and Kinematics of a New 3T1R Parallel Manipulator 2- (RPa3R) 3R with Zero Coupling and Motion Decoupling [J]. *Journal of Mechanical Engineering*, 2019, 55 (05): 53-64.
- [6] W Liu, H Z Liu. Synthesis of Parallel Mechanisms with 2T1R and 3R Motion Modes [J]. *Chinese Journal of Mechanical Engineering*, 2019, 55 (03): 53-63.
- [7] BHASKAR D, MRUTHYUNJAYA T S. A Newton-Euler formulation for the inverse dynamics of the Stewart platform manipulator[J]. *Mechanism and Machine Theory*, 1998, 33 (8): 1135-1152.
- [8] Naser M, Alireza A, Jaspreet D, et al. A comprehensive inverse dynamics problem of a Stewart platform by means of Lagrangian formulation[A]. *ASME 2017 Dynamic Systems and Control Conference*. Virginia: DSCC 2017-5098.
- [9] Y F Zhang, P Jin, J L Gong, Q Liu. Dynamic modeling of viscous friction conditions of 3-RPS parallel robot [J]. *Transactions of the Chinese Society of Agricultural Machinery*, 2018, 49 (09): 374- 381.
- [10] Y B Li, H Zheng, P Sun. Dynamic Modeling and Coupling Analysis of 5-PSS/UPU Parallel Mechanism Considering Joint Friction [J]. *Chinese Journal of Mechanical Engineering*, 2019, 55 (03) : 43-52.
- [11] Fu S, Yao Y, Wu Y. Comments on "A Newton-Euler formulation for the inverse dynamics of the Stewart platform manipulator"[J]. *Mechanism and Machine Theory*, 2007, 42, 1668-1671.
- [12] Pedrammehr S, Mahboubkhah M, Khani, N. Improved dynamic equations for the generally configured Stewart platform manipulator[J]. *Mechanical Science and Technology*. 2012, 26(3), 711-721.
- [13] X L Chen, W M Feng, Y S Zhao. Dynamic Model of a 5-DOF Parallel Robot Mechanism[J]. *Transactions of the Chinese Society of Agricultural Machinery*, 2013, 44 (01): 236-243.
- [14] M C Geng, T S Zhao, C Wang, et al. Dynamic analysis of 4-UPS/UPR parallel mechanism[J]. *Transactions of the Chinese Society of Agricultural Machinery*, 2014, 45 (8): 299-306.
- [15] Y G Li, Y M Song, Z Y Feng, C Zhang. Inverse dynamics analysis of 3-RPS parallel mechanism based on Newton's Euler method [J]. *Acta Aeronautica*, 2007 (05): 1210-1215.
- [16] S Z Liu, Y Q Yu, G N Tong, J X Yang. Kinematics and Dynamics Analysis of a 3 Degrees of Freedom Parallel Robot [J]. *Chinese Journal of Mechanical Engineering*, 2009, 45 (08): 11- 17
- [17] H P Shen, J M Deng, K Wang. A two translation and one rotation parallel mechanism with zero coupling and positive solution of analytical position, China, 201961623865x, 2019.6.11

Biographical notes

Ke Wang born in 1994, is currently an engineer at *Black & Decker(Suzhou) Technology Limited Company, China*. He received his master degree from *Changzhou University, China*, in 2020. E-mail: wangk1994@163.com

Ju Li, born in 1981, is currently a Vice Professor at *Changzhou University, China*. Her main research interests include parallel mechanism, kinematics, E-mail: wangju0209@163.com

Huiping Shen * born in 1965, is currently a professor and a PhD candidate supervisor at *Changzhou University, China*. His main research interests include parallel mechanism, kinematics, institutional topology.

E-mail: Shp65@126.com

Ting-Li Yang, born in 1940, is currently a guest professor at *Changzhou University, China*. His main research interest include modern mechanisms , basic theory of robotic mechanism.

Jingjing You, born in 1985, is currently a professor and a Master supervisor at *College of Mechanical and Electronic Engineering, Nanjing Forestry University, China*.

E-mail: youjingjing251010@126.com

E-mail: yangti@126.com

Figures

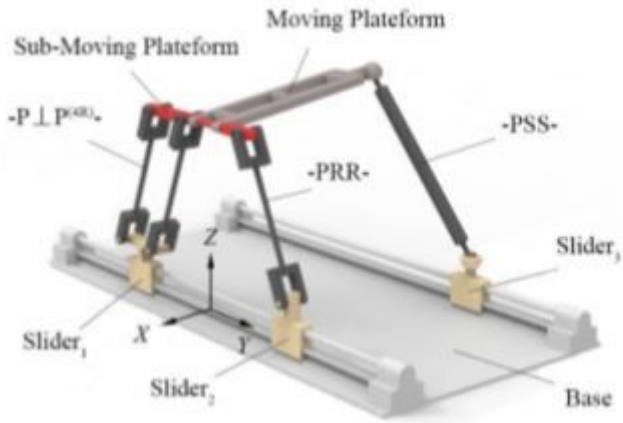


Figure 1

3D model of a 2T1R PM

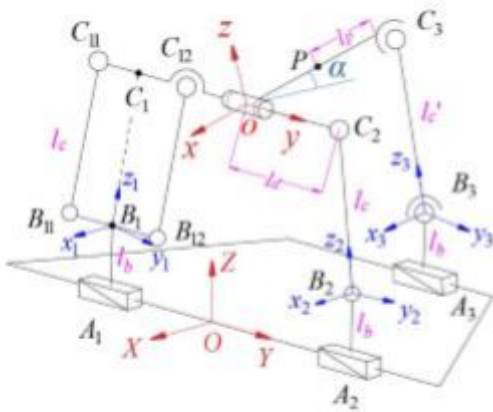


Figure 2

Schematic diagram of 2T1R PM

$${}^O R_{i3} = R(Y, \theta_1) R(x_3, \theta_2)$$

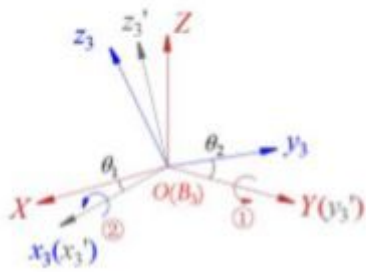


Figure 3

Coordinate system B3-x3y3z3 z Euler transform

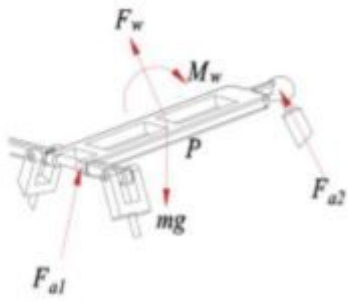


Figure 4

Force analysis of the moving platform

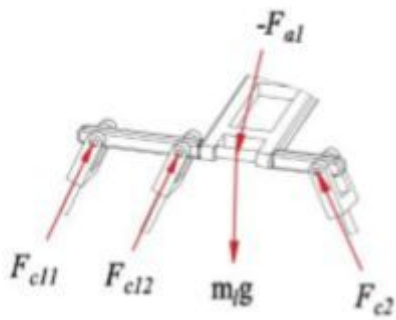


Figure 5

Force analysis of sub-moving platform

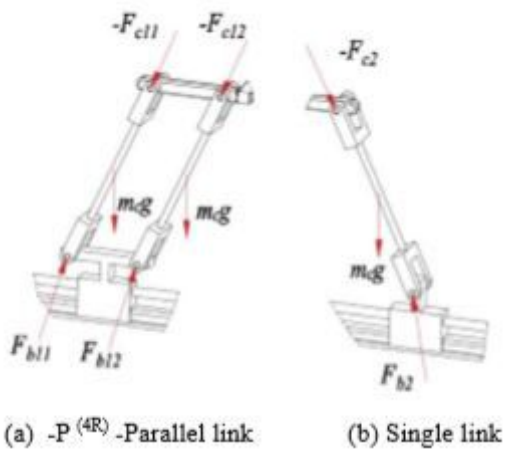


Figure 6

Force analysis of R-R-link



Figure 7

Force analysis diagram of S-S-Link

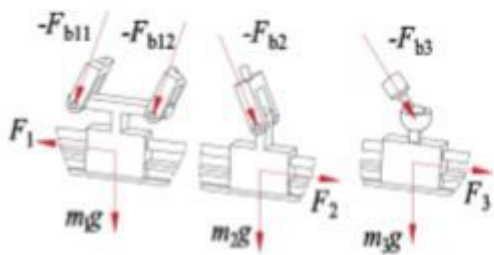


Figure 8

Force analysis of three drive sliders

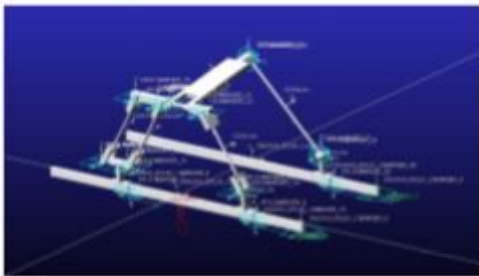
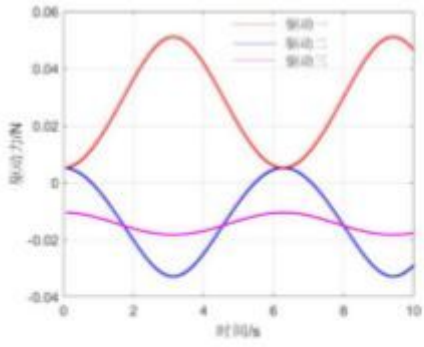
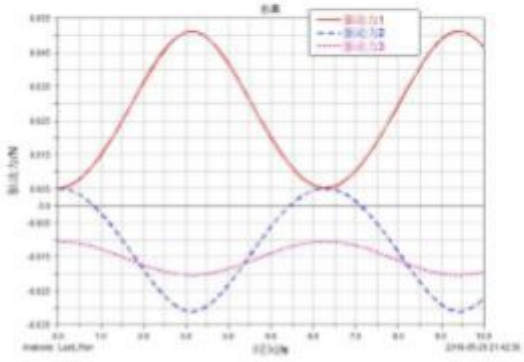


Figure 9

Virtual prototype of 2T1R parallel mechanism



(a) Theoretical driving force



(b) Driving force simulation value

Figure 10

Driving Force of Each Driving Pair